Pulse-spread minimization in single-mode optical fibers

G. R. Boyer
Laboratoire d'Optique Appliquée Ecole Polytechnique, Ecole Nationale Supérieure des Techniques Avancées, Batterie de l'Yvette, 91120 Palaiseau, France

X. F. Carlotti*
Centre de Mathématiques Appliquées, Ecole Polytechnique, 91128 Palaiseau Cédex, France
(Received 1 May 1987; revised manuscript received 13 June 1988)

The propagation of optical pulses in single-mode nonlinear dispersive fibers in the vicinity of the zero-dispersion wavelength has to take into account the third-order dispersion term. We show that, for short dispersion, the broadening of the pulses, described by the rms and full width at half maximum pulse width evolution, is reduced by a red shift from the zero-dispersion wavelength. Numerical resolution of the associated propagation equation, for initially 1.2-ps Gaussian pulses, shows that this spreading reduction remains valid to a few tenths of kilometers of propagation. Wavelength shift evaluations are obtained in a very simple way, by use of a moment expansion near the origin of propagation. A simple (nonexhaustive) explanation of the time-domain and Fourier-domain pulse evolution, based on the comparison of the phase velocities with the group and pulse mass-center velocities is proposed.

I. INTRODUCTION

Long-range propagation of short pulses in single-mode optical fibers has received considerable attention in the telecommunication domain. Enhancing both the range and bit rate is of particular interest. A long-range propagation involves high peak powers of the pulses, inducing self-phase modulation[1,2] (SPM) and dispersion effects. A balance between anomalous dispersion and SPM can be found, giving rise to the elegant soliton solution,[3–5] provided the loss term can be neglected. But this assumption is unrealistic for long-range links (50 km). Another way to lower the pulse spread is to make the carrier wavelength equal to the zero-dispersion wavelength (ZDWL). Some authors have recently shown[6–10] that, in this case, the third-order dispersion term cannot be neglected since the resulting spreading effects of this term increase with t^{-3}, where t is the full width at half maximum (FWHM) of the pulse. In this article, we point out that a small red shift from the ZDWL to a so-called optimized wavelength (OW) reduces significantly the pulse spread. It turns out that, even in the presence of an important third-order dispersion term, the second-order dispersion term partially balances the SPM effect. The OW is obtained by minimizing the increase of a second-order Taylor expansion of the rms pulse width around the origin of the propagation. Surprisingly, comparison of numerical resolutions of the propagation equation including the loss term, for the ZDWL and the OW, show that pulse spread minimization is valid even for distances over 50 km.

The existence of two successive propagation regimes may in both cases be deduced from the observation of the spectrum evolution: as mentioned recently,[11] an initially Gaussian spectrum splits into two bands; then after some distance of saturation, it remains stable. In the temporal domain, however, our numerical simulations show a splitting of the pulse into a stable leading peak and a trailing dispersive subpulse including multiple peaks. We show how these features are enhanced in the optimized propagation case. An interpretation based on the comparison of group velocity and mass-center velocity is proposed.

II. PULSE PROPAGATION EQUATION AND rms PULSE-WIDTH EVOLUTION

A. Envelope equation

A derivation of the pulse-envelope equation of the transverse electric field, using the slow-varying envelope approximation, has been proposed by previous authors;[12–14] this equation can be written in the form

$$\left[i\frac{\partial}{\partial z} - \frac{k_0''}{2}\frac{\partial^2}{\partial t^2} - \frac{i}{2}\left[\frac{k_0'''}{3} + \frac{k_0' k_0''}{k_0} \right] \frac{\partial^3}{\partial t^3} \right] A + \frac{n_2}{n_0} k_0 \left[1 + \frac{2i}{\omega_0}\frac{\partial}{\partial t} \right] |A|^2 A = 0 , \quad (2.1)$$

where $k^{(n)} = (\partial^n k / \partial \omega^n)_{\omega_0}$ and t is the reduced time.

The so-called nonlinear dispersive term $(\partial/\partial t)(|A|^2 A)$ (or shock term) is significant for subpicosecond pulses of a power level above 1 TW/cm^2. Such is the case of the optical pulse compression technique via the optical fiber compressor,[15–17] where the presence of this additional term in the nonlinear Schrödinger equation induces shock forming,[18] and a cubic term in the phase spectrum of the pulse.[19,20] Since we restrict our study to picosecond pulses, this shock term will not be taken into account. The propagation equation may be expressed in a nondimensional form. We denote by L, T, and P, the fiber length, the timewidth, and the peak power of the initial pulse, respectively. P is related to the peak amplitude E by

$$P=\tfrac{1}{2}n_0\left[\frac{\epsilon_0}{\mu_0}\right]^{1/2}|E|^2 . \tag{2.2}$$

We set

$$A=uE,\quad z=\xi L,\quad t=\tau T , \tag{2.3}$$

and obtain the nondimensional propagation equation

$$\frac{\partial u}{\partial \xi}=i\alpha\frac{\partial^2 u}{\partial \tau^2}+\beta\frac{\partial^3 u}{\partial \tau^3}+i\gamma|u|^2u , \tag{2.4}$$

where

$$\alpha=-\frac{k_0''}{2}\frac{L}{T^2} ,$$
$$\beta=\frac{1}{2}\left[\frac{k_0'''}{3}+\frac{k_0'k_0''}{k_0}\right]\frac{L}{T^3} , \tag{2.5}$$
$$\gamma=\frac{4\pi n_2}{\lambda n_0}\left[\frac{\mu_0}{\epsilon_0}\right]^{1/2}LP .$$

In the vicinity of the ZDWL, the expression of β is simplified,

$$\beta\simeq\frac{k_0'''}{6}\frac{L}{T^3} . \tag{2.6}$$

Relations (2.5) shows an increasing importance of the dispersion terms, especially the third-order one, with a decreasing time duration of the pulse.

B. Pulse spreading over short distances and optimization of the carrier wavelength

As we stated previously, the key point for a pulse-spread minimization is the choice of a wavelength, near the ZDWL, such that the second- and third-order dispersion terms cancel out at least partially the nonlinear term. That can be done by a derivation of the pulse rms near the origin of propagation.

First, let us set

$$C_j(\xi)=\int_{-\infty}^{+\infty}\left|\frac{\partial^j u}{\partial \xi^j}(\xi,\tau)\right|^2 d\tau , \tag{2.7}$$

$$M_k(\xi)=\int_{-\infty}^{+\infty}\tau^k|u(\xi,\tau)|^2 d\tau , \tag{2.8}$$

for $j,k=0,1,2$, and

$$k_0=\int_{-\infty}^{+\infty}|u_0(\xi,\tau)|^4 d\tau . \tag{2.9}$$

With these notations, the conservation of energy is written in the form

$$C_0(\xi)=C_0(\xi=0) . \tag{2.10}$$

Introducing the reduced meantime, the variance and the rms pulse width[7] gives, respectively, for a given propagation distance ξ

$$\langle\tau(\xi)\rangle=\frac{\int_{-\infty}^{+\infty}\tau|u(\xi,\tau)|^2 d\tau}{\int_{-\infty}^{+\infty}|u(\xi,\tau)|^2 d\tau}=\frac{M_1(\xi)}{C_0} , \tag{2.11}$$

$$\langle\tau^2(\xi)\rangle=\frac{\int_{-\infty}^{+\infty}\tau^2|u(\xi,\tau)|^2 d\tau}{\int_{-\infty}^{+\infty}|u(\xi,\tau)|^2 d\tau}=\frac{M_2(\xi)}{C_0} , \tag{2.12}$$

$$V(\xi)=\langle\tau^2(\xi)\rangle-\langle\tau(\xi)\rangle^2 , \tag{2.13}$$

$$\sigma(\xi)=V(\xi)^{1/2} . \tag{2.14}$$

We have demonstrated (see the Appendix) the following relations about the moments evolution:

$$\frac{d}{d\xi}\int_{-\infty}^{+\infty}\tau|u|^2 d\tau=3\beta\int_{-\infty}^{+\infty}\left|\frac{\partial u}{\partial \tau}\right|^2 d\tau , \tag{2.15a}$$

$$\frac{d^2}{d\xi^2}\int_{-\infty}^{+\infty}\tau^2|u^2|d\tau=-6\beta\gamma I_m\int_{-\infty}^{+\infty}u^2\left[\frac{\partial\bar{u}}{\partial\tau}\right]^2 d\tau , \tag{2.15b}$$

and

$$\frac{d^2}{d\xi^2}\int_{-\infty}^{+\infty}\tau^2|u|^2 d\tau=8\alpha^2\int_{-\infty}^{+\infty}\left|\frac{\partial u}{\partial\tau}\right|^2 d\tau-2\alpha\gamma\int_{-\infty}^{+\infty}|u|^4 d\tau-24i\alpha\beta\int_{-\infty}^{+\infty}\frac{\partial\bar{u}}{\partial\tau}\frac{\partial^2 u}{\partial\tau^2}d\tau$$
$$+18\beta^2\int_{-\infty}^{+\infty}\left|\frac{\partial^2 u}{\partial\tau^2}\right|^2 d\tau-12\beta\gamma\,\mathrm{Im}\int_{-\infty}^{+\infty}\tau u^2\left[\frac{\partial\bar{u}}{\partial\tau}\right]^2 d\tau . \tag{2.16}$$

Searching a pulse variance-minimizing scheme, we are able now to carry out from (2.14) and (2.15) a second-order Taylor expansion of $V(\alpha,\xi)$ around $\xi=0$ for a given value of α,

$$V(\alpha,\xi)=V_0+\xi\frac{\partial V}{\partial\xi}(\alpha,0)+\frac{\xi^2}{2}\frac{\partial^2 V(\alpha,0)}{\partial\xi^2}+O(\xi^3) . \tag{2.17}$$

For a real symmetric pulse, this expansion becomes

$$V(\alpha,\xi)=\frac{M_2(\alpha,0)}{C_0}+P_\gamma(\alpha)\xi^2+O(\xi^3) , \tag{2.18}$$

with

$$P_\gamma(\alpha)=4\alpha^2\frac{C_1}{C_0}-\alpha\gamma\frac{k_0}{C_0}+9\beta^2\left[\frac{C_2}{C_0}-\frac{C_1^2}{C_0^2}\right] . \quad (2.19)$$

The first term in (2.19) represents the second-order dispersion effect, the second one (negative in case of anomalous dispersion) the interplay of dispersion with nonlinear effects in the limit of the classical third-order expansion of the k^2 approximation, and the third term, describing the third-order dispersion effect, does not depend on the wavelength and is positive because of Schwarz's inequality

$$C_1^2 \le C_0 C_2 . \quad (2.20)$$

We focus our study on pulse-spreading optimization around the ZDWL regime, for which no soliton solution is aimed, and we seek to balance nonlinear self-phase modulation with second- and third-order dispersion terms, with the help of (2.18) and (2.19). It must be pointed out that second-order dispersion is now the perturbative term of the modified NLP equation with an additional third-order dispersion term. Taking the rms pulse width as a measure of the pulse duration may have some misleading effects, especially when a solitonlike solution causes the pulse to split into a stationary part, and a dispersively decaying linear pulse, giving rise to a linear variation of the associated rms pulse with respect to distance, giving undue weight to the decaying part. The study has to be completed by plotting the FWHM along the distance, in a similar way to previous work on soliton propagation in presence of chirp,[21] and for nontransform-limited pulses.[22] Moreover, the moments method summarized by relations (2.15), (2.16), and (2.17) is valid only near the origin, since conversely to the linear case,[23] it was not possible for us to derive the expressions for these quantities for any distance, unless a considerable amount of cumbersome algebra was used. Despite these restrictions, we estimate that it is relevant to derive a so-called optimized wavelength by use of the near-to-the-origin rms pulse minimization condition

$$\frac{dP_\gamma(\alpha)}{d\alpha}=0 , \quad (2.21)$$

leading to

$$\alpha=\alpha_{\rm opt}=\frac{k_0}{8C_1}\gamma , \quad (2.22)$$

and to observe afterward the pulse rms and the FWHM along the distance. This study is mainly centered on the relative importance on pulse spreading of second- and third-order dispersion. It is then useful to evaluate the ratio

$$R(\gamma)=\frac{4\alpha_{\rm opt}^2(C_1/C_0)-\alpha_{\rm opt}\gamma(k_0/C_0)}{9\beta^2[(C_2/C_0)-(C_1^2/C_0^2)]} , \quad (2.23)$$

and to consider the characteristic power $\bar{\gamma}$, for which

$$R(\bar{\gamma})=1 . \quad (2.24)$$

Making use of (2.22) gives

$$\bar{\gamma}=12\beta\left[\frac{C_0C_1}{k_0^2}\left[\frac{C_2}{C_0}-\frac{C_1^2}{C_0^2}\right]\right]^{1/2} . \quad (2.25)$$

All the constants appearing in this section have been computed for a Gaussian and a hyperbolic secant of width σ_0 and are given in Table I. For a 1-ps pulsewidth, $\bar{\gamma}$ is about 0.1 MW/cm^2.

Three propagation regimes can be considered. For small power ($\gamma \ll \bar{\gamma}$) principal dispersion dominates and (2.22) shows that $\alpha_{\rm opr}=0$; the optimal propagation is obtained for the ZDWL. Conversely, if $\gamma \gg \bar{\gamma}$, then $|R(\gamma)| \gg 1$; the third-order dispersion can be neglected so that Eq. (2.4) reduces to the nonlinear Schrödinger equation. Classically (2.5) and (2.22) show that dispersion is anomalous.[4] If $\gamma \simeq \bar{\gamma}$ both dispersion effects have to be considered in the study of the optimized propagation, some features of which are studied in Sec. III, on the basis of numerical simulations.

C. Comparison to previous results

The expression (2.18) can be interestingly compared with some known results of pulse propagation of solitons, perturbed solitons, and the ZDWL case.

1. Linear propagation

We want to show that when γ goes to zero, formulas (2.18) and (2.19) are equivalent to relation (34) of Ref. 7, when the source spectrum is assumed to be infinitely narrow ($W=0$). In the linear case, the C_j functions given by (2.7) are constant, so that relations (2.15) and (2.16) can be integrated over any distance. The variance is then given by

$$V(\alpha,\xi)=\sigma_0^2+\left[4\alpha^2\frac{C_1}{C_0}+g\beta^2\left[\frac{C_2}{C_0}-\frac{C_1^2}{C_0^2}\right]\right]\xi^2 . \quad (2.26)$$

Using Table I and with the help of formulas (2.5) and (2.6) we get, for an initially Gaussian pulse,

$$\sigma^2=\sigma_0^2\left[1+\frac{(k_0''z)^2}{(2T^2\sigma_0^2)^2}+\frac{1}{4}\frac{(k_0'''z)^2}{(2T^2\sigma_0^2)^3}\right] . \quad (2.27)$$

Comparing

$$u_0^2(\tau)=\exp\left[-\frac{\tau^2T^2}{2\sigma_0^2T^2}\right] \quad (2.28)$$

with relation (8) of Ref. 7 we see that Marcuse's time unit is $T\sigma_0\sqrt{2}$, so that (2.26) is identical to relation (34) of Ref. 7 when the source spectrum is assumed to be infinitely narrow ($W=0$).

2. Nonspreading condition for a Gaussian pulse and a hyperbolic secant when $\beta \ll \alpha$

It follows from (2.19) that, from λ_0 and in case of anomalous dispersion, the nonspreading condition is, for any pulse, given by

$$\frac{\gamma}{\alpha}=\frac{4C_1}{k_0} . \quad (2.29)$$

TABLE I. Characteristics constants for a Gaussian and a hyperbolic secant of energy pulsewidth σ_0.

	Gaussian	Hyperbolic secant	Pulse-shape ratio
		$u_0(\tau)=\mathrm{sech}(\tau/\tau_0)$,	
Definition	$u_0(\tau)=e^{-(\tau^2/4\sigma_0^2)}$	with $\tau_0=2\sqrt{3}\sigma_0/\pi$	
rms pulsewidth	σ_0	σ_0	1
C_0	$2\sigma_0\left[\frac{\pi}{2}\right]^{1/2}$	$2\tau_0$	$\frac{2\sqrt{2}}{\pi^{3/2}}\sqrt{3}\simeq 0.880$
C_1	$\frac{1}{2\sigma_0}\left[\frac{\pi}{2}\right]^{1/2}$	$\frac{2}{3\tau_0}$	$\frac{2\sqrt{2}}{3\sqrt{3}}\sqrt{\pi}\simeq 0.964$
C_2	$\frac{3}{(2\sigma_0)^3}\left[\frac{\pi}{2}\right]^{1/2}$	$\frac{14}{15}\tau_0^{-3}$	$\frac{\pi^{5/2}}{9\sqrt{3}}\frac{14}{15}\sqrt{2}\simeq 1.481$
$M_2(0)$	$2\sigma_0^3\left[\frac{\pi}{2}\right]^{1/2}$	$\frac{\pi^2}{6}\tau^3$	$\frac{2\sqrt{6}}{\pi^{3/2}}\simeq 0.880$
$4\frac{C_1}{C_0}$	σ_0^{-2}	$\frac{4}{3}\tau_0^{-2}$	$\left[\frac{\pi}{3}\right]^2\simeq 1.097$
$\frac{K_0}{C_0}$	$2^{-1/2}$	$\frac{2}{3}$	$\frac{2\sqrt{2}}{3}\simeq 0.943$
$9\left[\frac{C_2}{C_0}-\frac{C_1^2}{C_0^2}\right]$	$\frac{9}{8}\sigma_0^{-4}$	$\frac{16}{5}\tau_0^{-4}$	$\frac{2^3}{5}\left[\frac{\pi}{3}\right]^4\simeq 1.924$
$\alpha_{\mathrm{opt}}/\gamma$	$\sigma_0^2 2^{-1/2}$	$\frac{\tau_0^2}{2}$	$\frac{12}{\pi^2\sqrt{2}}\simeq 0.860$

Referring to the values of C_1 and k_0 given in Table I, we get for a Gaussian pulse

$$\left[\frac{\gamma}{\alpha}\right]_g=\frac{\sqrt{2}}{\sigma_0^2}\simeq\frac{1.41}{\sigma_0^2} \tag{2.30}$$

and for a hyperbolic secant

$$\left[\frac{\gamma}{\alpha}\right]_s=\frac{\pi^2}{6}\frac{1}{\sigma_0^2}\simeq\frac{1.64}{\sigma_0^2}\ . \tag{2.31}$$

Let us note that the fundamental soliton solution of Eq. (2.4), which is given by

$$u(\xi,\tau)=\frac{1}{\tau_0}\left[\frac{2\alpha}{\gamma}\right]^{1/2}\frac{1}{ch\left[\frac{\tau}{\tau_0}\right]}e^{i(\alpha/\tau_0^2)\xi} \tag{2.32}$$

and the condition

$$\frac{1}{\tau_0}\left[\frac{2\alpha}{\gamma}\right]^{1/2}=1 \tag{2.33}$$

is equivalent to (2.31).

3. *Solitonlike propagation with higher-order dispersion*

Making now $\beta\neq 0$ and setting $P_\gamma(\alpha)=0$ in (2.19), we get a steady pulse propagation condition in the presence of non-negligible second-order dispersion,

$$\frac{\gamma}{\alpha}=\frac{C_0}{k_0}\left[\frac{C_1}{C_0}+9\frac{\beta^2}{\alpha^2}\left[\frac{C_2}{C_0}-\frac{C_1^2}{C_0^2}\right]\right]\ . \tag{2.34}$$

For such a value of the ratio γ/α, the variance, considered a function of the distance ξ, is a constant if we neglect a third-order term,

$$V(\xi)=V^0+O(\xi^3)\ . \tag{2.35}$$

The first-order term is zero because the initial pulse shape has been assumed to be symmetrical; the second-order term is zero because of the condition (2.33).

The nonspreading value of the ratio γ/α increases with β, because both dispersion terms have to be compensated. For large values of the ratio β/α, it behaves like $(\beta/\alpha)^2$.

It is relevant to consider the carrier wavelength for which the power given by (2.34) takes its minimal value. Such a power is given by

$$\gamma_{\min}=6\beta\left[\frac{C_1C_0}{k_0^2}\left[\frac{C_2}{C_0}-\frac{C_1^2}{C_0^2}\right]\right]^{1/2}, \tag{2.36}$$

which leads, for a Gaussian pulse of pulsewidth σ_0, to

$$\gamma_{\min}\sigma_0^3=\frac{\beta}{2} \tag{2.37}$$

(see Table I). We get then from (2.5) the peak power required from a solitonlike propagation,

$$P(\sigma_0 T)^3=f\frac{\epsilon n_0 c\lambda k_0'''}{\pi n_2}\ , \tag{2.38}$$

where the dimensionless coefficient f is equal to $\frac{1}{16}\simeq 0.06$. This can be compared to formulas (8)–(10) of Ref. 11, which give $f\geq 0.24$. These formulas have been obtained by a very different method, so that we only retain that these two values of the minimal power have the same or-

der of magnitude. If we used maximal pulse contraction as in (2.21) and Ref. 24, our value of f should be multiplied by a factor of 2.

III. NUMERICAL RESULTS

The pulse-propagation equation (2.4) is solved numerically by means of the widely used split-step Fourier algorithm:[13,25] the nonlinear step is solved analytically, and the dispersive step by using the FFT. Convergence has been checked by increasing the number of samples in the FFT and the number of steps.

As an example, we consider the propagation over 50 km of a 1.2-ps, 0.2-MW/cm^2 Gaussian pulse. The coefficients of Eq. (2.4) are then given by

$$\alpha=0.52, \quad \beta=0,123, \quad \gamma=5.90 . \tag{3.1}$$

The value of α corresponds to a wavelength shift $\lambda_{opt}-\lambda_0=\delta\lambda$ of 1.2 nm. Such a propagation has been compared to the ZDWL case, for which $\alpha=0$ in (3.1). In this section, the results have been given without any loss term. Figure 1 shows the compared peak power evolution between the optimized, critical, and linear cases (curves 1, 2, and 3, respectively). Curve 1 exhibits a compression near the origin, a consequence of condition (2.22). Figure 2 shows the pulse rms (curves *a*, *b*, and *c*), and the FWHM (curve 1, 2, and 3) for the same optimized, critical, and linear cases, respectively. In Fig. 2 two successive regimes can be observed: regime I, characterized by the interplay of nonlinear and dispersive effects, inducing a nonlinear variation of the rms pulsewidth, and regime II, dominated by dispersion for which the increase of the rms pulse width becomes linear with propagation distance. This feature has already been noted.[6,7] Classically, the slopes are higher in nonlinear propagation because the spectrum broadening occurring in regime I increases the dispersion effects in regime II.

Figures 3 and 4 show the temporal and spectral profiles for increasing distances, respectively, for critical and op-

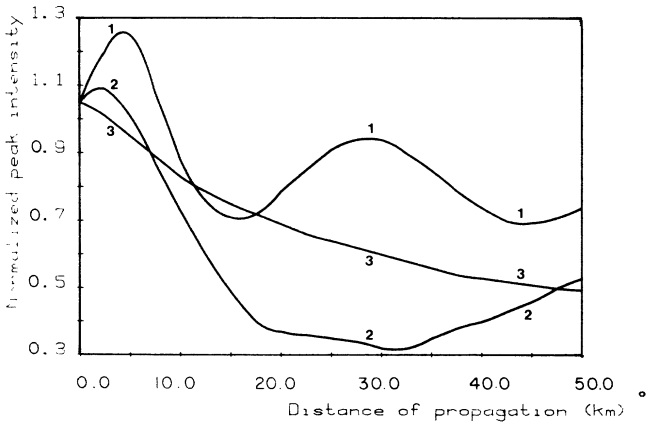

FIG. 1. Normalized peak intensity variations along the distance of propagation (in km) of an initially 1.2-ps, 0.2-MW/cm Gaussian pulse in a lossless monomode fiber for the optimized and critical wavelengths curves 1 and 2, and for the linear case 3.

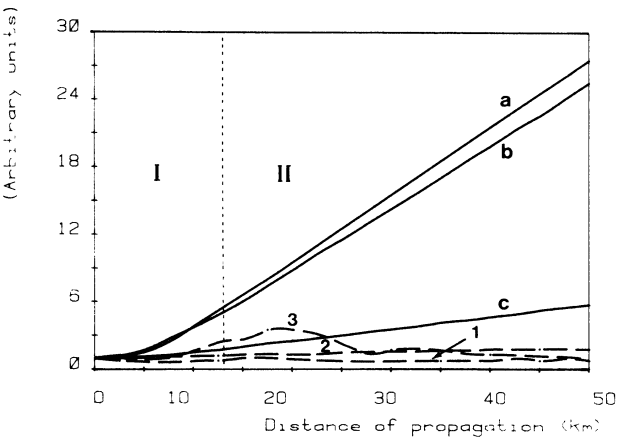

FIG. 2. Normalized rms (solid line; curves *a*, *b*, and *c*) and FWHM (dotted line; curves 1, 2, and 3), for the optimized and critical wavelengths and for the linear case, respectively. The pulse parameters are the same as in Fig. 1.

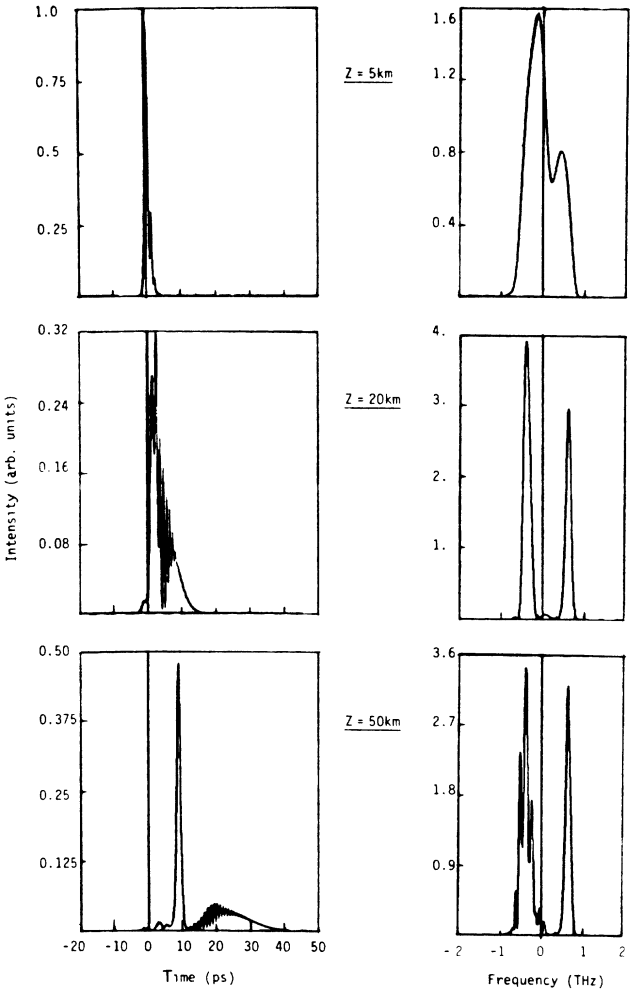

FIG. 3. Normalized temporal and spectral evolution at the critical wavelength of the pulse defined in Fig. 1.

timized propagations. Curves related to a 5-km distance are characteristic of regime I. After 10 km, regime II is reached, characterized by a quasitable spectrum. For the critical dispersion propagation case (Fig. 3), the initially Gaussian pulse splits into two parts; the leading part is a slowly decreasing peak of stable FWHM that remains almost centered at the origin of the reduced time frame. The trailing part exhibits some ringing and spreads out regularly. The spectrum splits gradually into two bands, a result at least qualitatively consistent with Fig. 5 of Ref. 8, where the same oscillating structure and the same splitting characteristics are observed.

Figure 4 represents the optimized propagation features. The temporal profile fits the general characteristics mentioned above; we note, however, a higher, narrower, and more stable main peak than in the critical case, while the trailing edge spreads faster and is under 1% of the main peak power after 10 km. In the spectral domain, the two bands are no longer symmetric, and the red side band is close to the central frequency. As clearly shown by comparison of temporal profiles in Figs. 3 and 4, the widening of the pulses is significantly reduced, especially for the distance of 20 km, the subpulses are flattened by a larger amount, and the peak power remains higher for the optimized propagation.

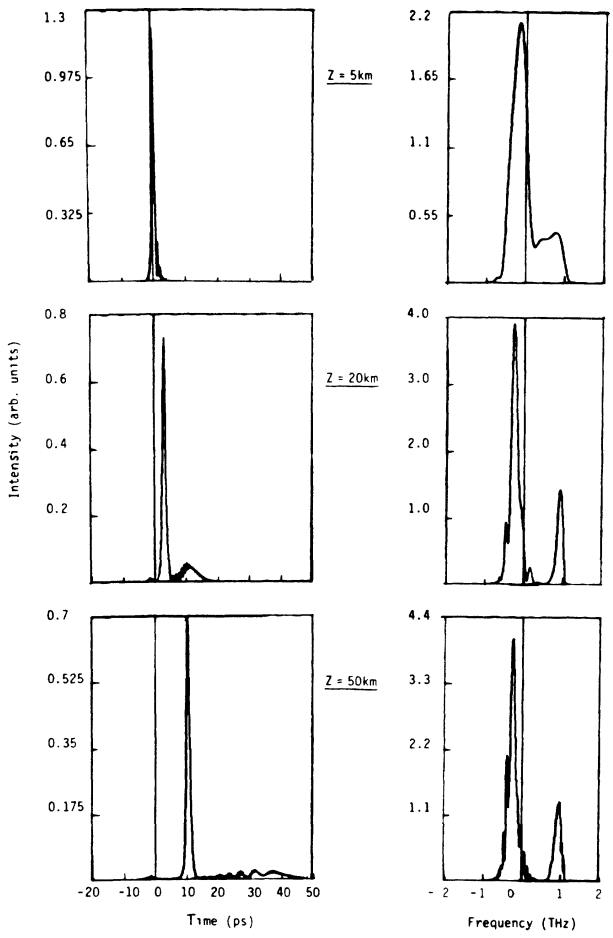

FIG. 4. Normalized temporal and spectral evolution at the optimized wavelength of a pulse defined in Fig. 1.

A. Interpretation of the observed pulse distortion

The splitting of the spectrum suggests an interpretation of the numerical results, involving the mass center velocity.

1. Simple model

Figure 5 shows a linear increasing of the mean reduced time in regime II. We get from (2.35a)

$$\bar{\tau}(\xi)-\bar{\tau}(\xi_0)=3\beta\frac{C_1}{C_0}(\xi-\xi_0)\ , \tag{3.2}$$

where ξ_0 is the reaching distance of regime II.

The mean time is then given by

$$\bar{t}(z)-\bar{t}(z_0)=\frac{z-z_0}{v_g}+3\beta\frac{C_1}{C_0}\frac{z-z_0}{L}T\ . \tag{3.3}$$

The mass-center velocity, defined as

$$v_{cg}=\frac{z-z_0}{\bar{t}(z)-\bar{t}(z_0)}\ , \tag{3.4}$$

is then bound to the group velocity v_g by

$$\frac{v_g}{v_{cg}}=1+3\beta\frac{C_1}{C_0}\frac{v_gT}{L}\ . \tag{3.5}$$

Let us study (Fig. 6) the intersection points of the reduced phase velocities curve

$$v_\varphi(\omega)=\frac{\omega-\omega_0}{k-k_0}\ , \tag{3.6}$$

with v_{cg} in both cases of critical and optimized regimes (curves *A* and *B*).

The abscissa values $\omega_0+\delta\omega_{+,-}$ of these points are the

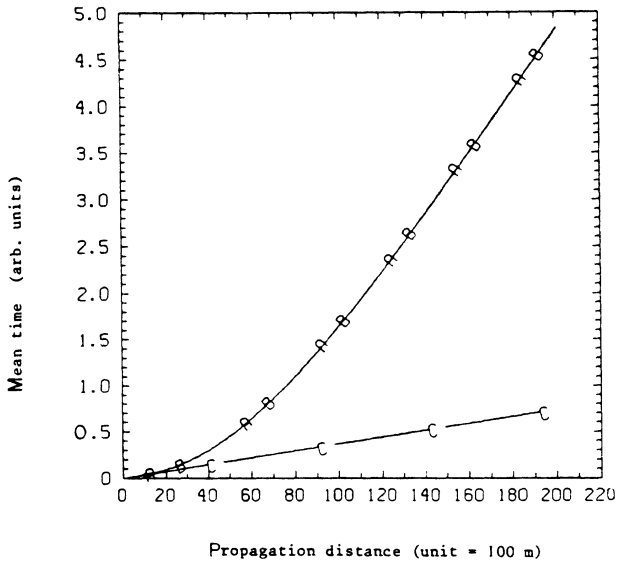

FIG. 5. Mean for the critical and optimized propagation (curves *A* and *B*); the corresponding linear case is shown in curve *C*.

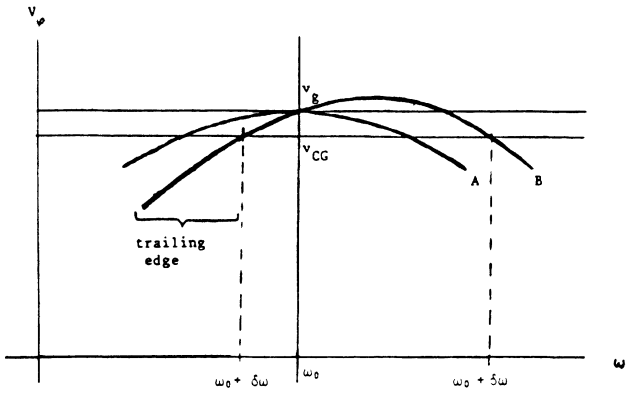

FIG. 6. Phase velocity curves v for critical and optimized values of the group velocity dispersion parameter. Curve A, $\lambda=\lambda_0$ (ZDWL); curve B, $\lambda=\lambda_0+\delta\lambda$ (OW) linear case (curve C).

two spectral peak frequencies, provided the other spectrum components can be neglected. Their algebraic expressions can be obtained by expanding $k(\omega)$ around ω_0 up to the third order, so that

$$v_\varphi(\omega)=\frac{v_g}{1-\frac{\delta\omega}{2}\left[-\frac{k_0''}{k_0'}\right]+\frac{\delta\omega^2}{6}\frac{k_0'''}{k_0'}}\ ; \tag{3.7}$$

$\delta\omega_+$ and $\delta\omega_-$ are then the roots of the equation,

$$(T\delta\omega)^2-\frac{\alpha}{\beta}(T\delta\omega)-3\frac{C_1}{C_0}=0\ . \tag{3.8}$$

Expressing these roots gives

$$\delta\omega_+=T^{-1}\left\{\frac{\alpha}{2\beta}\pm\left[\left[\frac{\alpha}{2\beta}\right]^2+3\frac{C_1}{C_0}\right]^{1/2}\right\}. \tag{3.9}$$

The asymptotic value of the coefficient C_1/C_0 is given by the slope of the reduced mean time [see (3.2) and Fig. 5].

These values have been compared to those obtained by numerical integration (Figs. 3 and 4) (see Table II). The discrepancy between two couples of values can be explained by the fact that the simple model involves only two spectral lines and not a continuum of frequencies.

We may note that if β is zero, then $v_g=v_{cg}$. Then the only intersection point of $v_\varphi(\omega)$ with v_{cg} (Fig. 6) is given by $\omega=\omega_0$. It is known that, in this case, the spectrum exhibits a single peak. As a result, this simple model shows the role of the mass center velocity and permits us to explain the structure of the spectrum in various cases of nonlinear dispersive propagation.

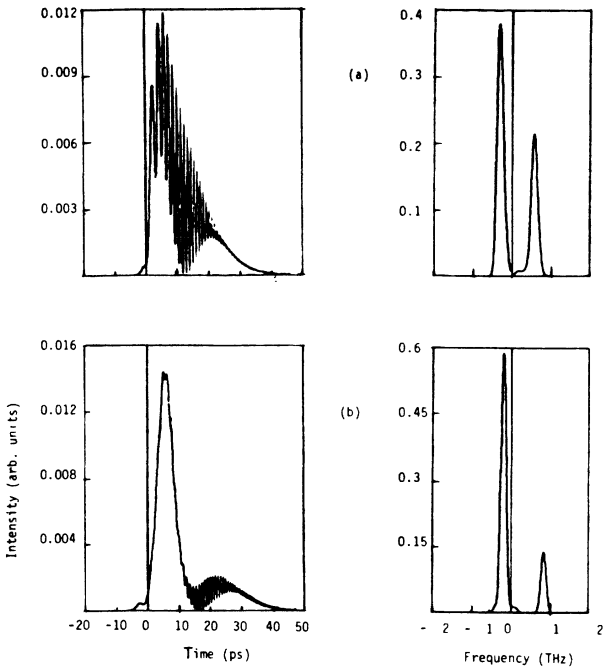

FIG. 7. Comparison of critical and optimized propagations at $z=50$ km, for a loss coefficient of 0.2 db/km.

2. *Optimized dispersion physical interpretation*

The main features of optimized propagation can be understood through the previous simple model. Figure 6 shows curve A to be tangent to v_g, while curve B exhibits a wider range of frequencies approximately moving at the group velocity. The main subpulse, moving at the group velocity (Fig. 4) is then more intense and stable.

Moreover, looking at the left-hand side of Fig. 6, we see that in the domain of frequencies moving more slowly than the mass center, curve B has a steeper slope than curve A. This explains the faster spreading of the trailing edge, in the optimized propagation case.

The subpulse preceding the main pulse (Fig. 4) is related to the presence in curve B (Fig. 5) of a spectral band moving faster than v_g.

B. Loss effects

For a better understanding of the interplay between dispersion and nonlinearity, we have, in a first step, neglected the loss term effects.[24,26] The results presented above have to be reviewed by introducing in the propagation-evolution equation (2.1) a 0.2 dB/km loss

TABLE II. Spectrum peak abscissa values in asymptotical configuration.

	Critical case (THz)		Optimized case (THz)	
	$\delta\omega_-$	$\delta\omega_+$	$\delta\omega_-$	$\delta\omega_+$
Two-spectral-line approx.	−0.8	0.8	−0.5	1.2
Numerical integration	−0.4	0.6	−0.2	1

term. The pulse evolution in an absorptive medium is presented in Figs. 7(a) and 7(b) (critical and optimized propagations).

We observe that the asymptotical regime is reached faster because of the weakening of the nonlinear effects. Comparison of Figs. 7(a) and 7(b), however, shows that the optimization remains valid.

IV. CONCLUSION

We have considered the problem of minimizing optical pulse distortion in nonlinear dispersive fibers, in the vicinity of the zero-dispersion wavelength. Derivation of differential expressions of the mean time and the rms permitted us to study the variations of the rms pulse width for which an expansion has been given for short distances. We have then shown that, for a given amount of secondary dispersion and peak power, a red shift of the wavelength from the ZDWL permitted to reduce significantly the pulse spreading both in the rms and FWHM sense. This wavelength shift introduces a second-order dispersion effect increasing with the pulse power. Comparing the two dispersion effects led us to define a characteristic power P, depending on the third-order dispersion and the pulse duration. The case $P \simeq \bar{P}$ has been investigated here, and it turned out that a shift of the carrier frequency leads the pulse to propagate with reduced side lobes and spreading.

Examination of the pulse spectrum suggests a physical interpretation of this phenomena, based on the mass-center pulse velocity concept, that accounts for qualitative results related to critical and optimized propagation.

The method, based on the properties of the rms pulse width for small distances, actually remains valid for long-range propagation, even in the presence of a loss term in the propagation equation.

For given values of the timewidth and peak power, an optimal wavelength, slightly above the ZDWL, has thus been defined. The peak power is found to be above the power of the fundamental soliton of same timewidth and carrier frequency. Moreover, the corresponding pulse profile splits into two subpulses: a main, leading, stable pulse, analogous to the fundamental soliton pulse, and a trailing, dispersive, fast-spreading subpulse. These features can be found even in the presence of a large secondary dispersion term.

ACKNOWLEDGMENTS

We wish to thank Professor A. Bamberger for valuable advice. The graphic processing of the results have been achieved with the help of the Centre Interrégional de Calcul Electronique (France).

APPENDIX: DIFFERENTIAL EXPRESSIONS (2.15)–(2.16) OF THE FIRST- AND SECOND-ORDER MOMENTA

For a given real function ψ, we multiply the evolution equation (2.4) by $\psi\bar{u}$, integrate over the time variable τ, and take the real part of the result. We obtain

$$\frac{1}{2}\frac{d}{d\xi}\int \psi |u|^2 d\tau = \alpha \,\mathrm{Im}\int \frac{d\psi}{d\tau}\bar{u}\frac{\partial u}{\partial \tau}d\tau + \beta\left[\frac{3}{2}\int \frac{d\psi}{d\tau}\left|\frac{\partial u}{\partial \tau}\right|^2 d\tau - \frac{1}{2}\int \frac{d^3\psi}{d\tau^3}|u|^2 d\tau\right]. \quad \text{(A1)}$$

Deriving (2.4) with regard to τ and using the same procedure leads to

$$\frac{1}{2}\frac{d}{d\xi}\int \psi\left|\frac{\partial u}{\partial \tau}\right|^2 d\tau = \alpha\,\mathrm{Im}\int \frac{d\psi}{d\tau}\frac{d\bar{u}}{\partial \tau}\frac{\partial^2 u}{\partial \tau^2}d\tau + \beta\left[\frac{3}{2}\int \frac{d\psi}{d\tau}\left|\frac{\partial^2 u}{\partial \tau^2}\right|^2 d\tau - \frac{1}{2}\int \left|\frac{d^3\psi}{d\tau^3}\right|\left|\frac{\partial u}{\partial \tau}\right|^2 d\tau\right] - \gamma\,\mathrm{Im}\int \psi u^2\left[\frac{\partial \bar{u}}{\partial \tau}\right]^2 d\tau. \quad \text{(A2)}$$

Moreover, a second conservation law is available,

$$\mathrm{Im}\int_{-\infty}^{+\infty}\bar{u}\frac{\partial u}{\partial \tau}d\tau = \text{const}, \quad \text{(A3)}$$

which follows from the relations

$$\frac{d}{d\xi}\left[i\int_{-\infty}^{+\infty}\bar{u}\frac{\partial u}{\partial \tau}d\tau\right] = -\mathrm{Im}\int_{-\infty}^{+\infty}\frac{\partial u}{\partial \xi}\frac{\partial u}{\partial \tau}d\tau$$

and

$$\mathrm{Im}\left[\frac{\partial u}{\partial \xi}\frac{\partial \bar{u}}{\partial \tau}\right] = \beta\,\mathrm{Im}\left[\frac{\partial^3 u}{\partial \tau^3}\frac{\partial \bar{u}}{\partial \tau}\right] + \gamma\frac{\partial}{\partial \tau}G(u),$$

with

$$G(u) = \frac{\alpha}{2}\left|\frac{\partial u}{\partial \tau}\right|^2 + \frac{\gamma}{4}|u|^4.$$

Applying then formulas (A1) with $\psi(\tau)=\tau$ and (A2) with $\psi(\tau)=1$ leads to (2.15a) and (2.15b).

Proof of (2.16) is obtained by substituting $\psi(\tau)=\tau^2$ in (A1). We obtain

$$\frac{1}{2}\frac{d}{d\xi}\int_{-\infty}^{+\infty}\tau^2|u|^2 d\tau = 2\alpha\,\mathrm{Im}\int_{-\infty}^{+\infty}\tau\bar{u}\frac{\partial u}{\partial \tau}d\tau + 3\beta\int_{-\infty}^{+\infty}\tau\left|\frac{\partial u}{\partial \tau}\right|^2 d\tau$$

and

$$\frac{d^2}{d\xi^2}\int_{-\infty}^{+\infty}\tau^2|u|^2 d\tau = 4\alpha\frac{d}{d\xi}\left[\mathrm{Im}\int_{-\infty}^{+\infty}\tau\bar{u}\frac{\partial u}{\partial \tau}d\tau\right] + 6\beta\frac{d}{d\xi}\int_{-\infty}^{+\infty}\tau\left|\frac{\partial u}{\partial \tau}\right|^2 d\tau. \quad \text{(A4)}$$

The first term in (A4), equal to $4\alpha T_1$, with

$$T_1 = 2\,\mathrm{Im}\int \tau \frac{\partial u}{\partial \tau}\frac{\partial \bar{u}}{\partial \xi}d\tau - \mathrm{Im}\int \bar{u}\frac{\partial u}{\partial \xi}d\tau\ ,$$

is evaluated by expressing $\partial u/\partial \xi$ with the help of (2.4), which leads to

$$T_1 = 2\alpha\int\left|\frac{\partial u}{\partial \tau}\right|^2 d\tau - 3i\beta\int \frac{\partial u}{\partial \tau}\frac{\partial^2 u}{\partial \tau^2}d\tau - \frac{\gamma}{2}\int |u|^4 d\tau\ .$$

The second term in (A4), equal to $6\gamma T_2$, is then evaluated by means of (A2) with $\psi(\tau)=\tau$, which gives

$$T_2 = \frac{d}{d\xi}\int \tau\left|\frac{\partial u}{\partial \tau}\right|^2 d\tau = 2\alpha\,\mathrm{Im}\int \frac{\partial u}{\partial \tau}\frac{\partial^2 \bar{u}}{\partial \tau^2}d\tau + 3\beta\int\left|\frac{\partial^2 u}{\partial \tau^2}\right|^2 d\tau - 2\gamma\,\mathrm{Im}\int \tau u^2\left[\frac{\partial \bar{u}}{\partial \tau}\right]^2 d\tau\ .$$

This proves (2.16).

---

*Present address: Commissariat à l'Energie Atomique, Centre de Vaujours, Boîte Postale No. 7, 77181 Courtry, France.

[1]F. Shimizu, Phys. Rev. Lett. **19**, 1097 (1967).
[2]R. H. Stolen, and C. Lin, Phys. Rev. A **17**, 1448 (1978).
[3]V. E. Zakharov and A. B. Shabat, Zh. Eksp. Teor. Fiz. **61**, 118 (1971) [Sov. Phys.–JETP **34**, 62 (1972)].
[4]A. Hasegawa and F. Tappert, Appl. Phys. Lett. **23**, 142 (1973).
[5]F. L. Mollenauer, R. H. Stolen, and J. P. Gordon, Phys. Rev. Lett. **45**, 1095 (1980).
[6]V. A. Vysloukh, Kvant. Elektron. (Moscow) **10**, 1688 (1983) [Sov. J. Quantum Electron. **13**, 1113 (1983)].
[7]D. Marcuse, Appl. Opt. Lett. **19**, 1653 (1980).
[8]G. P. Agrawal, M. J. Potasek, Phys. Rev. A **33**, 1765 (1986).
[9]M. J. Potasek, G. P. Agrawal, and S. C. Pinault, J. Opt. Soc. Am. B **3**, 205 (1986).
[10]G. R. Boyer and X. F. Carlotti, Opt. Commun. **60**, 18 (1986).
[11]P. K. A. Wai, C. R. Menyuk, M. H. Chen, and Y. C. Lee, Opt. Lett. **12**, 628 (1987).
[12]N. Tzoar and M. Jain, Phys. Rev. A **23**, 1266 (1981).
[13]R. A. Fisher and W. K. Bischel, J. Appl. Phys. **46**, 4921 (1975).
[14]T. K. Gustafson, J. P. Taran, H. A. Haus, J. R. Lifsitz, and P. Kelley, Phys. Rev. **177**, 306 (1969).
[15]W. J. Tomlinson, R. H. Stolen, and C. V. Shank, J. Opt. Soc. Am. **2**, 139 (1984).
[16]W. H. Knox, R. L. Fork, M. C. Downer, R. H. Stolen, C. V. Shank, and J. A. Valdmanis, Appl. Phys. Lett. **46**, 1120 (1985).
[17]B. Niklolaus and D. Grischkowsky, Appl. Phys. Lett. **42**, 1 (1983).
[18]E. Bourkoff, W. Zhao, R. I. Joseph, and D. N. Christodoulides, Opt. Commun. **62**, 284 (1987).
[19]E. Bourkoff, W. Zhao, R. I. Joseph, and D. N. Christodoulides, Opt. Lett. **12**, 272 (1987).
[20]D. Anderson and M. Lisak, Phys. Rev. A **17**, 1393 (1983).
[21]H. E. Lassen, F. Mengel, B. Tromborg, N. C. Albertsen, and P. L. Christiansen, Opt. Lett. **10**, 34 (1985).
[22]K. J. Blow and D. Wood, Opt. Commun. **58**, 349 (1986).
[23]D. Anderson and M. Lisak, Phys. Rev. A **35**, 184 (1987).
[24]A. Hasegawa and Y. Kodama, Proc. IEEE **69**, 1145 (1981).
[25]D. Yevik and B. Hermanson, Opt. Commun. **47**, 101 (1983).
[26]K. J. Blow and N. J. Doran, Opt. Commun. **42**, 403 (1982).